Spin excitation anisotropy in the optimally isovalent-doped superconductor $BaFe_2(As_{0.7}P_{0.3})_2$

Ding Hu,[1,2,3,*] Wenliang Zhang,[3,4] Yuan Wei,[3,4] Bertrand Roessli,[5] Markos Skoulatos,[5,6] Louis Pierre Regnault,[7]
Genfu Chen,[3,4,8] Yu Song,[1] Huiqian Luo,[3] Shiliang Li,[3,4,8] and Pengcheng Dai[1,2,†]

[1]*Department of Physics and Astronomy, Rice University, Houston, Texas 77005-1827, USA*

[2]*Center for Advanced Quantum Studies and Department of Physics, Beijing Normal University, Beijing 100875, China*

[3]*Beijing National Laboratory for Condensed Matter Physics, Institute of Physics, Chinese Academy of Sciences, Beijing 100190, China*

[4]*School of Physical Sciences, University of Chinese Academy of Sciences, Beijing 100190, China*

[5]*Laboratory for Neutron Scattering and Imaging, Paul Scherrer Institut, CH-5232 Villigen, Switzerland*

[6]*Heinz Maier-Leibnitz Zentrum (MLZ) and Physics Department E21, Technische Universität München, D-85748 Garching, Germany*

[7]*Institut Laue Langevin, 71 Avenue des Martyrs, 38042 Grenoble, France*

[8]*Collaborative Innovation Center of Quantum Matter, Beijing, China*

We use neutron polarization analysis to study spin excitation anisotropy in the optimally isovalent-doped superconductor $BaFe_2(As_{0.7}P_{0.3})_2$ ($T_c = 30$ K). Different from optimally hole- and electron-doped $BaFe_2As_2$, where there is a clear spin excitation anisotropy in the paramagnetic tetragonal state well above T_c, we find no spin excitation anisotropy for energies above 2 meV in the normal state of $BaFe_2(As_{0.7}P_{0.3})_2$. Upon entering the superconducting state, significant spin excitation anisotropy develops at the antiferromagnetic (AF) zone center $\mathbf{Q}_{AF} = (1,0,L = \text{odd})$, while the magnetic spectrum is isotropic at the zone boundary $\mathbf{Q} = (1,0,L = \text{even})$. By comparing the temperature, wave vector, and polarization dependence of the spin excitation anisotropy in $BaFe_2(As_{0.7}P_{0.3})_2$ and hole-doped $Ba_{0.67}K_{0.33}Fe_2As_2$ ($T_c = 38$ K), we conclude that such anisotropy arises from spin-orbit coupling and is associated with the nearby AF order and superconductivity.

DOI: 10.1103/PhysRevB.96.180503

Spin-orbit coupling (SOC) is an interaction of an electron's spin with its motion. While the importance of SOC to the electronic properties of the $4d$ and $5d$ correlated electron materials such as Sr_2RuO_4 and Sr_2IrO_4 is long recognized [1,2], its relevance to the physics of the $3d$ correlated electron materials such as iron pnictide superconductors is much less clear. Since iron pnictide superconductors are derived from metallic parent compounds exhibiting antiferromagnetic (AF) order at T_N below a tetragonal-to-orthorhombic structural transition temperature T_s associated with orbital ordering and nematic phase [Fig. 1(a)] [3–7], most microscopic theories for iron-based superconductors are focused on the role of spin [8–10], orbital [11], or nematic [7,12] fluctuations to the electron pairing and superconductivity. Although angle-resolved photoemission spectroscopy (ARPES) experiments on different families of iron-based superconductors have identified the presence of SOC through observation of electronic band splitting at the Brillouin zone center (ZC) below T_s [13–15], much is unknown concerning the role of SOC to the AF order, nematic phase, electron pairing mechanism, and superconductivity [16–19].

In addition to its impact on the Fermi surface and electronic band dispersions, SOC also brings lattice anisotropies into anisotropies of magnetic fluctuations [20,21], as seen from nuclear magnetic resonance [22] and polarized inelastic neutron scattering (INS) experiments on different iron-based superconductors [23–34]. Compared with ARPES measurements, polarized INS measurements have much better energy and momentum resolution, and can directly probe the energy, wave vector, and temperature dependence of the spin excitation

anisotropy and determine its relationship with T_c, T_N, T_s, and nematic phase. For hole-doped $Ba_{1-x}K_xFe_2As_2$ [35–38], electron-doped $BaFe_{2-x}TM_xAs_2$ (TM = Co, Ni) [39–42], and isovalent-doped $BaFe_2(As_{1-x}P_x)_2$ [43–45] superconductors, unpolarized INS experiments found that superconductivity is coupled with the appearance of a low-energy collective spin excitation mode termed spin resonance that has superconducting order parameter-like temperature dependence below T_c [46–51]. Although polarized INS experiments have conclusively established the presence of SOC induced low-energy spin excitation anisotropy near the resonance mode in different families of iron-based superconductors [23–34], the spin excitation anisotropy persists in the paramagnetic tetragonal state, and becomes isotropic at temperatures well above T_N and T_s [25,26,30–32]. Therefore, it is still unclear how SOC is coupled to spin fluctuation anisotropy and superconductivity.

To resolve this problem, we used polarized INS to study low-energy spin excitations in optimally isovalent-doped $BaFe_2(As_{0.7}P_{0.3})_2$ ($T_c = 30$ K; Fig. 1), where superconductivity induces a resonance of $E = 9$ meV at $\mathbf{Q}_{AF} = (1,0,1)$ that disperses to $E = 12$ meV at $\mathbf{Q} = (1,0,0)$ (Fig. 2) [50,51]. We chose $BaFe_2(As_{0.7}P_{0.3})_2$ because the system has no AF order and structural distortion [45], and is believed to be near a magnetic [44] or a nematic quantum critical point [12]. Since the AF order in $BaFe_2(As_{1-x}P_x)_2$ is gradually suppressed with increasing x similar to electron- and hole-doped $BaFe_2As_2$ [45], one would expect low-energy spin excitations in $BaFe_2(As_{0.7}P_{0.3})_2$ to behave similarly to those of optimally doped $BaFe_{2-x}TM_xAs_2$ and $(Ba,K)Fe_2As_2$, and exhibit anisotropy at temperatures well above T_c [25,26,32]. Surprisingly, we find that spin excitations are completely isotropic in spin space above T_c for energies above 2 meV. Upon entering into the superconducting state, spin excitations
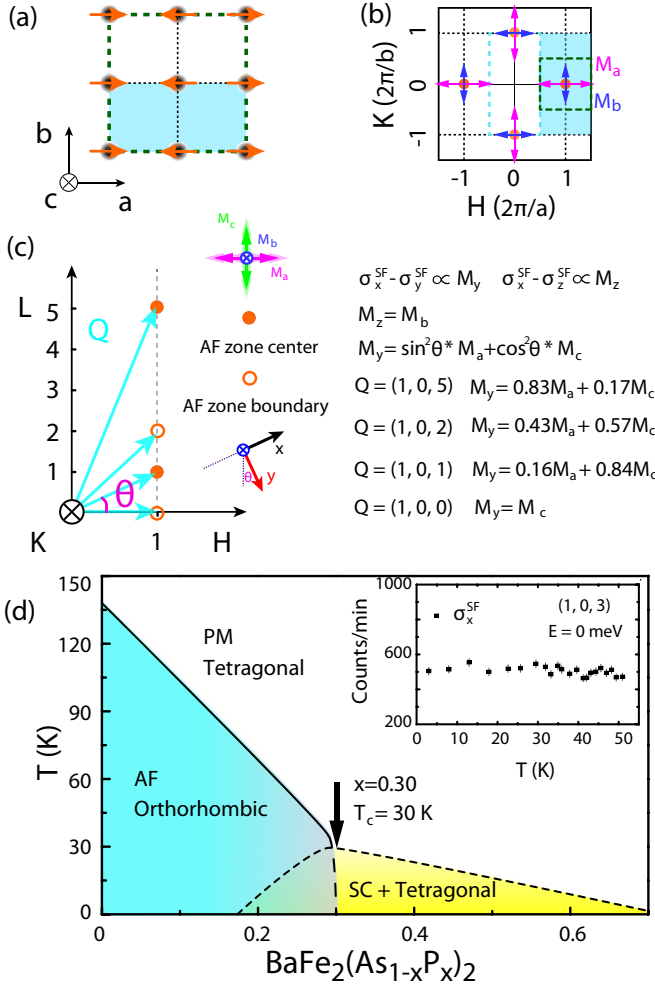
*dinghuphys@gmail.com
†pdai@rice.edu

FIG. 1. (a) Chemical (dotted line with the orthorhombic lattice parameters of a, b, and c) and magnetic (cyan area) unit cells of $BaFe_2As_2$ in the AF orthorhombic phase. The arrows depict the stripe magnetic structure with ordered moments aligned along the a axis. (b) The reciprocal space of $BaFe_2As_2$, where orange dots indicate in-plane AF ordering wave vector (Q_{AF}). The presence of a magnetic peak at $(0,\pm1)$ is due to twinning. Magenta and blue arrows indicate spin excitations polarized along the in-plane longitudinal (M_a) and transverse (M_b) directions. (c) $[H,0,L]$ scattering plane used in this experiment. Cyan arrows indicate the measured $\mathbf{Q}$, the solid orange dots are the AF ZCs, and the orange circles are at the zone boundaries along the c axis. Neutron polarization directions ($\alpha = x, y, z$) and deduced three components ($M_{a,b,c}$) of magnetic excitations are marked by colored arrows. The equations show the relationship of $M_{a,b,c}$ and σ_α^{NSF} at different wave vectors. (d) The schematic electronic phase diagram of $BaFe_2(As_{1-x}P_x)_2$ [45]. The black arrow marks $BaFe_2(As_{0.70}P_{0.30})_2$ in the phase diagram. No AF order is found at the $Q_{AF} = (1,0,3)$ position as shown in the inset.

FIG. 2. Energy scans for the neutron SF channels under different neutron polarization directions, marked as $\sigma_{x,y,z}^{SF}$, at $T = 2$ K and $\mathbf{Q} = (1,0,L)$ for (a) $L = 1$, (b) $L = 5$, (d) $L = 0$, (e) $L = 2$; and (c) at 35 K with $\mathbf{Q} = (1,0,1)$. (f) The neutron SF scattering σ_x^{SF} at $T = 2$ K with $L = 1$, and 0.

at $Q_{AF} = (1,0,1)$ become anisotropic, with the a-axis polarized resonance extending to the lowest energy ($M_a \gtrsim 3$ meV), followed by c-axis ($M_c \gtrsim 5$ meV) and b-axis ($M_b \gtrsim 6$ meV) polarized modes (Figs. 3 and 4). The resonance and spin excitation anisotropy vanish around T_c. Although superconductivity also induces a resonance at $\mathbf{Q} = (1,0,0)$, it is isotropic with $M_a \approx M_b \approx M_c$ [Figs. 2(d), 2(e) and
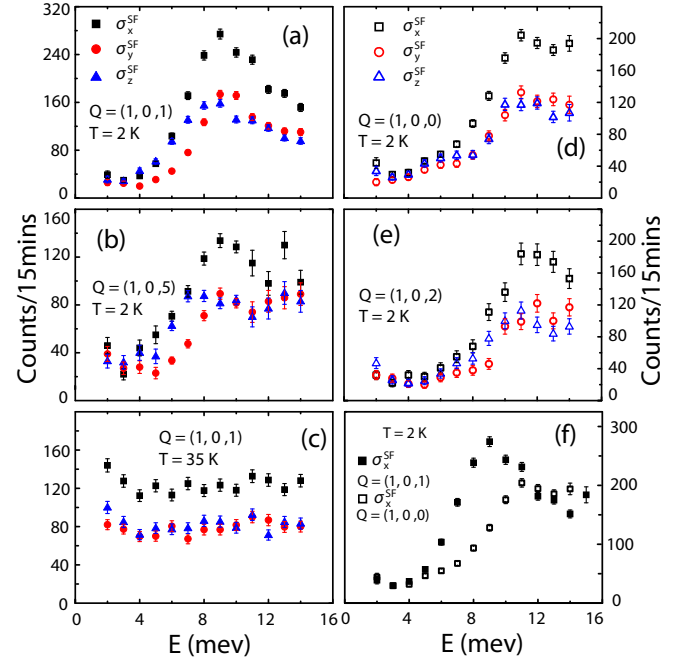
3(e)–3(h)]. These results thus indicate that the spin excitation anisotropy in $BaFe_2(As_{0.7}P_{0.3})_2$ is closely related to the static AF order and superconductivity. Assuming that SOC in iron pnictides gives rise to magnetic single-ion anisotropy that controls the ordered moment direction in the AF ordered phase [28,29], the dramatic temperature dependence of the spin excitation anisotropy across T_c with negligible modification of the lattice suggests a direct association of SOC with magnetic fluctuations inside the superconducting state [52].

Figure 1(b) shows the reciprocal space of magnetically ordered $BaFe_2As_2$ [Fig. 1(a)], where the magnitudes of spin excitations polarized along the a-, b-, and c-axis directions at $Q_{AF} = (1,0,1)$ are marked as M_a, M_b, and M_c, respectively. Our high-quality $BaFe_2(As_{0.7}P_{0.3})_2$ single crystals were grown by a self-flux method as described previously [45]. We have coaligned 17-g single crystals in the $[H,0,L]$ scattering plane with an in-plane mosaic $<7°$. A polarized INS experiment was performed using the triple-axis spectrometer IN22 at the Institut Laue-Langevin, Grenoble, France, using a CRYOPAD as described previously [26]. In such an experiment, the incident neutron beam is polarized along the momentum transfer $\mathbf{Q}$ direction (x) or two perpendicular directions (y,z) as shown in Fig. 1(c). Neutron spin-flip (SF) and non-spin-flip (NSF) scattering cross sections for each polarization can then be written as σ_α^{SF} and σ_α^{NSF} ($\alpha = x, y, z$), respectively. The leakage between SF and NSF channels can be quantified by the neutron spin flipping ratio $R = \sigma_\alpha^{NSF}/\sigma_\alpha^{SF}$ for a nuclear Bragg peak [27]. For the experiments, we find $R = 16$ for all neutron polarizations. By carrying out neutron polarization analysis at $Q_{AF} = (1,0,L = 1,5)$ and $\mathbf{Q} = (1,0,L = 0,2)$ with σ_α^{SF}, we can determine the magnitude of magnetic scattering M_a, M_b,
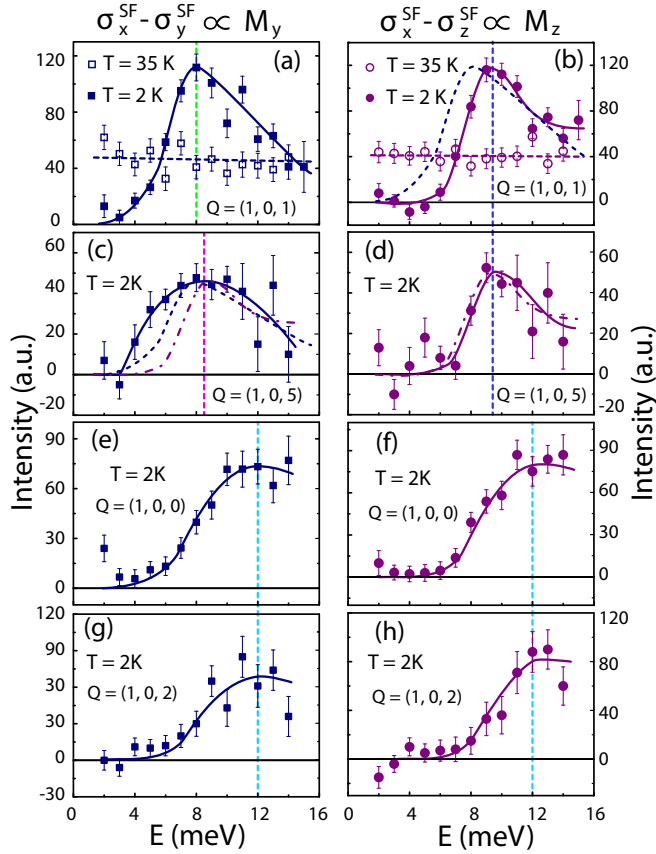
FIG. 3. The differences between σ_x^{SF} and $\sigma_{y,z}^{\mathrm{SF}}$ at different $\mathbf{Q} = (1,0,L)$ and temperatures. (a), (b) $L = 1$. (c), (d) $L = 5$. (e), (f) $L = 0$. (g), (h) $L = 2$. The solid lines are guides to the eye. The dashed and dashed-dotted lines in (b-d) are the solid lines in (a) and (b), respectively.

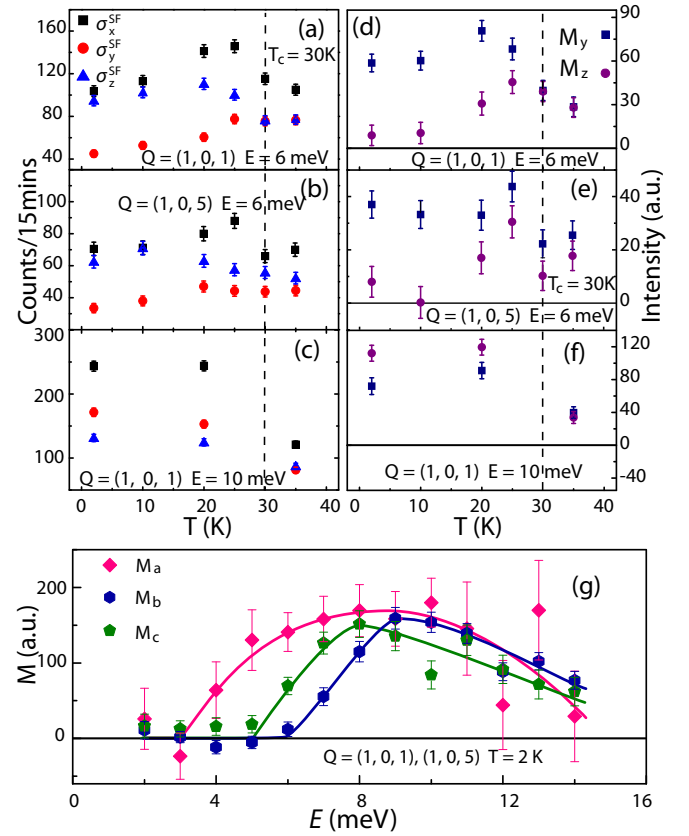
FIG. 4. Temperature dependence of $\sigma_{x,y,z}^{\mathrm{SF}}$ at (a) $\mathbf{Q}(= 1,0,1)$ and $E = 6$ meV, (b) $\mathbf{Q} = (1,0,5)$ and $E = 6$ meV, and (c) $\mathbf{Q} = (1,0,1)$ and $E = 10$ meV. (d)–(f) show the corresponding M_y and M_z. (g) The energy dependence M_a, M_b, and M_c at $T = 2$ K obtained using data in Figs. 2(a) and 2(b) [27]. The vertical dashed lines mark T_c. The solid lines are guides to the eye.

and M_c via $(\sigma_x^{\mathrm{SF}} - \sigma_y^{\mathrm{SF}})/c = M_y = M_a \sin^2\theta + M_c \cos^2\theta$ and $(\sigma_x^{\mathrm{SF}} - \sigma_z^{\mathrm{SF}})/c = M_z = M_b$, where $c = (R-1)/(R+1)$ and θ is the angle between $\mathbf{Q} = (1,0,L)$ and $(1,0,0)$ [Fig. 1(c)] [6]. As measurements of $\sigma_\alpha^{\mathrm{SF}}$ at $\mathbf{Q}_{\mathrm{AF}} = (1,0,1)$ can only give M_y and M_z, a conclusive determination of M_a and M_c requires data at more than one AF ZC positions [Fig. 1(c)] [26].

In previous unpolarized INS experiments on the optimally P-doped $\mathrm{BaFe_2(As_{1-x}P_x)_2}$ superconductor, the neutron spin resonance is found to be dispersive along the c axis, suggesting a close connection of the mode to the three-dimensional AF spin correlations [50,51]. Figures 2(a) and 2(b) show raw data of $\sigma_\alpha^{\mathrm{SF}}$ in the superconducting state ($T = 2$ K) at $\mathbf{Q}_{\mathrm{AF}} = (1,0,1)$ and $\mathbf{Q}_{\mathrm{AF}} = (1,0,5)$, respectively. For isotropic paramagnetic scattering with the same background in different channels, one would expect $(\sigma_x^{\mathrm{SF}} - \mathrm{BG})/2 = \sigma_y^{\mathrm{SF}} - \mathrm{BG} = \sigma_z^{\mathrm{SF}} - BG$. While the data show a clear resonance around 9 meV for all three neutron polarization directions (x,y,z), there are clear differences between σ_y^{SF} and σ_z^{SF} below 10 meV. For energies below 3 meV, there is no magnetic scattering due to the opening of a spin gap in response to superconductivity ($\sigma_x^{\mathrm{SF}} = \sigma_y^{\mathrm{SF}} = \sigma_z^{\mathrm{SF}}$). On warming to $T = 35$ K above T_c, the scattering becomes featureless down to 2 meV with $\sigma_x^{\mathrm{SF}}/2 \approx \sigma_y^{\mathrm{SF}} = \sigma_z^{\mathrm{SF}}$ consistent with the scattering being isotropic [Fig. 2(c)]. These results are clearly different

from those of hole- [30–32] and electron-doped [23,25,26] $\mathrm{BaFe_2As_2}$.

Figures 2(d) and 2(e) show $\sigma_\alpha^{\mathrm{SF}}$ below T_c at the AF zone boundary positions $\mathbf{Q} = (1,0,0)$ and $\mathbf{Q} = (1,0,2)$, respectively. While the data shows a clear resonance around 12 meV and a spin gap below 6 meV, we find $\sigma_x^{\mathrm{SF}}/2 \approx \sigma_y^{\mathrm{SF}} \approx \sigma_z^{\mathrm{SF}}$ at all other energies indicative of isotropic scattering. The dispersive nature of the resonance is clearly seen by overplotting σ_x^{SF} at $\mathbf{Q}_{\mathrm{AF}} = (1,0,1)$ and $\mathbf{Q} = (1,0,0)$ [Fig. 2(f)] [51].

To gain insight into the spin excitation anisotropy from $\sigma_\alpha^{\mathrm{SF}}$, we calculate the energy dependence of M_y and M_z at different L values, corresponding to different sensitivity to M_a and M_c [Fig. 1(c)]. Figures 3(a) and 3(b) show the energy dependence of M_y and M_z at $\mathbf{Q}_{\mathrm{AF}} = (1,0,1)$ below and above T_c. In the normal state, both M_y and M_z are featureless in the measured energy range. Although superconductivity induces a resonance for both channels around 9 meV, the energy width of the resonance is narrower in M_z, resulting in a smaller spin gap for M_y. At $\mathbf{Q}_{\mathrm{AF}} = (1,0,1)$, $M_y = 0.16 M_a + 0.84 M_c$ and is therefore mostly sensitive to M_c. These results suggest that the c-axis polarized resonance extends to lower energies than the b-axis polarized resonance [53]. Figures 3(c) and 3(d) plot the energy dependence of M_y and M_z at $\mathbf{Q}_{\mathrm{AF}} = (1,0,5)$

below T_c. As $M_z = M_b$ is independent of L, we would expect identical energy dependence for scans at $\mathbf{Q}_{AF} = (1,0,1)$ and $\mathbf{Q}_{AF} = (1,0,5)$ aside from minor differences due to instrumental resolution and the Fe magnetic form factor [27]. Inspection of Figs. 3(b) and 3(d) finds this to indeed be the case. On the other hand, since $M_y = 0.83M_a + 0.17M_c$ at $\mathbf{Q}_{AF} = (1,0,5)$, M_y in Fig. 3(c) should be mostly sensitive to the a-axis polarized spin excitations. Compared with Figs. 3(a) and 3(b), Fig. 3(c) reveals that the shape of M_a sensitive resonance is different from M_b and M_c with a broader peak and a spin gap of 3 meV. Figures 3(e)–3(h) summarize the energy dependence of M_y and M_z at the AF zone boundaries of $\mathbf{Q} = (1,0,0)$ and $(1,0,2)$ positions. Consistent with Figs. 2(d) and 2(e), these scans confirm the isotropic nature of spin excitations at the AF zone boundary.

Given the clear experimental evidence for anisotropic spin excitations at the AF ZC below T_c and its absence above T_c, it would be interesting to determine the temperature dependence of the spin excitation anisotropy. Figure 4(a) shows the temperature dependence of σ_α^{SF} at 6 meV and $\mathbf{Q}_{AF} = (1,0,1)$. The corresponding M_y and M_z are shown in Fig. 4(d). Since M_y is dominated by M_c at this wave vector and $M_z = M_b$, superconductivity induces magnetic anisotropy at 6 meV by enhancing M_c and suppressing M_b. Similarly, the temperature dependence of the magnetic scattering σ_α^{SF} at 6 meV and $\mathbf{Q}_{AF} = (1,0,5)$ in Fig. 4(b) reveals that superconductivity also enhances M_a and suppresses M_b [Fig. 4(e)]. Figure 4(c) plots the temperature dependence of σ_α^{SF} at 10 meV and $\mathbf{Q}_{AF} = (1,0,1)$. From the resulting M_y and M_z [Fig. 4(f)], we see that superconductivity induces a weakly anisotropic M_c and M_b resonance at 10 meV.

Based on measurements of spin excitation anisotropies at $\mathbf{Q}_{AF} = (1,0,1)$ and $(1,0,5)$ in Figs. 1(c) and 2, we deduce the energy dependence of M_a, M_b, and M_c in the super-conducting state as shown in Fig. 4(g) [26,27]. The order of resonance energies for different polarization directions in $BaFe_2(As_{0.7}P_{0.3})_2$ is reminiscent of the spin anisotropy in weakly Co-doped NaFeAs, where the a axis corresponds to the direction of ordered moment and is lowest in energy, followed by spin waves polarized along the c and b axes [27]. This suggests spin anisotropy resulting from SOC in $BaFe_2(As_{0.7}P_{0.3})_2$ remains similar to a superconducting sample coexisting with static AF order [27], in contrast to $Ba_{0.67}K_{0.33}Fe_2As_2$ in which the c-axis polarized resonance is the lowest in energy [32]. For comparison, we note that spin excitation anisotropy in $BaFe_2As_2$ in the AF ordered state has M_c in the lowest energy, followed by M_b, and M_a [29,54]. In the paramagnetic state of $BaFe_2As_2$, M_a diverges around T_N [54]. Our observation is in line with the phase diagram of P- and K-doped $BaFe_2As_2$; whereas stripe magnetic order with ordered moment along the a axis is observed near optimal superconductivity in $BaFe_2(As_{1-x}P_x)_2$ [45], a double-$\mathbf{Q}$ phase with ordered moments along the c axis is seen near optimal superconductivity in $Ba_{1-x}K_xFe_2As_2$ [36–38]. Our data also suggests a progressively reduced integrated spectral weight of the resonance for M_a, M_c, and M_b. Since paramagnetic scattering of $BaFe_2(As_{0.7}P_{0.3})_2$ is isotropic in the normal state, our results suggest that the a-axis polarized resonance induced by superconductivity gains the maximum spectrum weight, followed by c-axis and b-axis polarized resonance modes

[Fig. 4(g)], in qualitative agreement with theoretical results that consider SOC [20].

In general, the symmetries of the crystallographic lattice can induce anisotropies in spin space that can determine the magnetic ordered moment direction. For iron pnictides that display a tetragonal-to-orthorhombic lattice distortion at T_s, orbital ordering in the low-temperature orthorhombic phase is believed to play an important role in determining the a-axis moment direction of the collinear AF ordered phase [21]. When $BaFe_2As_2$ is doped with P to form superconducting $BaFe_2(As_{0.7}P_{0.3})_2$, the static AF order and orthorhombic lattice distortion of the parent compounds are completely suppressed, similar to optimally hole-doped $Ba_{0.67}K_{0.33}Fe_2As_2$ [49]. Given that both pnictides are near optimal superconductivity with no orthorhombic lattice distortion and static AF order, orbital or nematic ordering associated with lattice distortion cannot play a direct role for the observed spin excitation anisotropy [21]. However, if we assume that the resonance arises from hole and electron Fermi surface nesting [8], the presence of SOC [13] may induce hole- and electron-doping asymmetry, giving rise to a double-$\mathbf{Q}$ tetragonal AF structure with ordered moments along the c axis near optimally hole-doped $Ba_{1-x}K_xFe_2As_2$ and a simple collinear AF structure for electron-doped iron pnictides [18]. Since AF ordered $BaFe_2(As_{1-x}P_x)_2$ also has a simple collinear magnetic structure [45], one would expect the low-energy spin excitations in $Ba_{0.67}K_{0.33}Fe_2As_2$ and $BaFe_2(As_{0.7}P_{0.3})_2$ to be c-axis and a-axis polarized, respectively, as our experiments reveal. Similarly, low-energy spin excitations in $NaFe_{0.985}Co_{0.015}As$ contain a significant a-axis polarized component, reflective of the collinear AF structure of underdoped $NaFe_{1-x}Co_xAs$ with the a axis being the easy axis [27]. For comparison, recent polarized INS experiments reveal that the resonance and the normal-state spin fluctuations in FeSe are anisotropic and have a strong c-axis polarized component [34].

The absence of spin anisotropy in the normal state of $BaFe_2(As_{0.7}P_{0.3})_2$ may be related to less quenched disorder compared with the K- and Ni-doped $BaFe_2As_2$, and is also consistent with the Curie-Weiss elastoresistance seen all the way down to T_c [12]. The significant spin excitation anisotropy at $\mathbf{Q}_{AF} = (1,0,1)$ below T_c and $E \leqslant 10$ meV suggests a stronger out-of-plane effective coupling relative to single-ion anisotropy energies in $BaFe_2(As_{0.7}P_{0.3})_2$ as compared to $Ba_{0.67}K_{0.33}Fe_2As_2$ [53]. Since spin excitation anisotropy is already present in the normal state of electron- and hole-doped iron pnictide superconductors, one cannot uniquely determine the effect of superconductivity to spin excitation anisotropy. The absence of spin excitation anisotropy in the normal state and its appearance below T_c at the AF ZC $\mathbf{Q}_{AF} = (1,0,1)$ in $BaFe_2(As_{0.7}P_{0.3})_2$ provide the most compelling evidence that superconductivity is coupled with SOC induced spin excitation anisotropy, and such anisotropy is associated with the nearby AF order and can occur for iron pnictides with the negligible lattice distortion [52].

---

[1] M. W. Haverkort, I. S. Elfimov, L. H. Tjeng, G. A. Sawatzky, and A. Damascelli, Phys. Rev. Lett. **101**, 026406 (2008).

[2] B. J. Kim, H. Jin, S. J. Moon, J.-Y. Kim, B.-G. Park, C. S. Leem, J. Yu, T. W. Noh, C. Kim, S.-J. Oh, J.-H. Park, V. Durairaj, G. Cao, and E. Rotenberg, Phys. Rev. Lett. **101**, 076402 (2008).

[3] Y. Kamihara, T. Watanabe, M. Hirano, and H. Hosono, J. Am. Chem. Soc. **130**, 3296 (2008).

[4] C. de la Cruz, Q. Huang, J. W. Lynn, J. Li, W. Ratcliff II, J. L. Zarestky, H. A. Mook, G. F. Chen, J. L. Luo, N. L. Wang, and P. C. Dai, Nature (London) **453**, 899 (2008).

[5] D. C. Johnston, Adv. Phys. **59**, 803 (2010).

[6] P. C. Dai, Rev. Mod. Phys. **87**, 855 (2015).

[7] R. M. Fernandes, A. V. Chubukov, and J. Schmalian, Nat. Phys. **10**, 97 (2014).

[8] P. J. Hirschfeld, M. M. Korshunov, and I. I. Mazin, Rep. Prog. Phys. **74**, 124508 (2011).

[9] D. J. Scalapino, Rev. Mod. Phys. **84**, 1383 (2012).

[10] Q. Si, R. Yu, and E. Abrahams, Nat. Rev. Mater. **1**, 16017 (2016).

[11] H. Kontani and S. Onari, Phys. Rev. Lett. **104**, 157001 (2010).

[12] H.-H. Kuo, J.-H. Chu, J. C. Palmstrom, S. A. Kivelson, and I. R. Fisher, Science **352**, 958 (2016).

[13] S. V. Borisenko, D. V. Evtushinsky, Z.-H. Liu, I. Morozov, R. Kappenberger, S. Wurmehl, B. Bühner, A. N. Yaresko, T. K. Kim, M. Hoesch, T. Wolf, and N. D. Zhigadlo, Nat. Phys. **12**, 311 (2016).

[14] P. D. Johnson, H.-B. Yang, J. D. Rameau, G. D. Gu, Z.-H. Pan, T. Valla, M. Weinert, and A. V. Fedorov, Phys. Rev. Lett. **114**, 167001 (2015).

[15] M. D. Watson, T. K. Kim, A. A. Haghighirad, N. R. Davies, A. McCollam, A. Narayanan, S. F. Blake, Y. L. Chen, S. Ghannadzadeh, A. J. Schofield, M. Hoesch, C. Meingast, T. Wolf, and A. I. Coldea, Phys. Rev. B **91**, 155106 (2015).

[16] K. Seo, J. D. Sau, and S. Tewari, Phys. Rev. B **95**, 205107 (2017).

[17] O. Vafek and A. V. Chubukov, Phys. Rev. Lett. **118**, 087003 (2017).

[18] M. H. Christensen, J. Kang, B. M. Andersen, I. Eremin, and R. M. Fernandes, Phys. Rev. B **92**, 214509 (2015).

[19] R. M. Fernandes and O. Vafek, Phys. Rev. B **90**, 214514 (2014).

[20] M. M. Korshunov, Y. N. Togushova, I. Eremin, and P. J. Hirschfeld, J. Supercond. Nov. Magn. **26**, 2873 (2013).

[21] R. Applegate, R. R. P. Singh, C.-C. Chen, and T. P. Devereaux, Phys. Rev. B **85**, 054411 (2012).

[22] Z. Li, D. L. Sun, C. T. Lin, Y. H. Su, J. P. Hu, and G.-Q. Zheng, Phys. Rev. B **83**, 140506(R) (2011).

[23] O. J. Lipscombe, L. W. Harriger, P. G. Freeman, M. Enderle, C. L. Zhang, M. Y. Wang, T. Egami, J. P. Hu, T. Xiang, M. R. Norman, and P. C. Dai, Phys. Rev. B **82**, 064515 (2010).

[24] K. Prokeš, A. Hiess, W. Bao, E. Wheeler, S. Landsgesell, and D. N. Argyriou, Phys. Rev. B **86**, 064503 (2012).

[25] P. Steffens, C. H. Lee, N. Qureshi, K. Kihou, A. Iyo, H. Eisaki, and M. Braden, Phys. Rev. Lett. **110**, 137001 (2013).

[26] H. Q. Luo, M. Wang, C. L. Zhang, X. Y. Lu, L.-P. Regnault, R. Zhang, S. L. Li, J. P. Hu, and P. C. Dai, Phys. Rev. Lett. **111**, 107006 (2013).

[27] C. L. Zhang, Y. Song, L.-P. Regnault, Y. X. Su, M. Enderle, J. Kulda, G. T. Tan, Z. C. Sims, T. Egami, Q. Si, and P. C. Dai, Phys. Rev. B **90**, 140502 (2014).

[28] N. Qureshi, P. Steffens, S. Wurmehl, S. Aswartham, B. Büchner, and M. Braden, Phys. Rev. B **86**, 060410 (2012).

[29] C. Wang, R. Zhang, F. Wang, H. Q. Luo, L. P. Regnault, P. C. Dai, and Y. Li, Phys. Rev. X **3**, 041036 (2013).

[30] C. L. Zhang, M. S. Liu, Y. X. Su, L.-P. Regnault, M. Wang, G. T. Tan, Th. Brückel, T. Egami, and P. C. Dai, Phys. Rev. B **87**, 081101 (2013).

[31] N. Qureshi, C. H. Lee, K. Kihou, K. Schmalzl, P. Steffens, and M. Braden, Phys. Rev. B **90**, 100502 (2014).

[32] Y. Song, H. R. Man, R. Zhang, X. Y. Lu, C. L. Zhang, M. Wang, G. T. Tan, L.-P. Regnault, Y. X. Su, J. Kang, R. M. Fernandes, and P. C. Dai, Phys. Rev. B **94**, 214516 (2016).

[33] F. Waßer, C. H. Lee, K. Kihou, P. Steffens, K. Schmalzl, N. Qureshi, and M. Braden, Sci. Rep. **7**, 10307 (2017).

[34] M. Ma, P. Bourges, Y. Sidis, Y. Xu, S. Li, B. Hu, J. Li, F. Wang, and Y. Li, Phys. Rev. X **7**, 021025 (2017).

[35] M. Rotter, M. Tegel, and D. Johrendt, Phys. Rev. Lett. **101**, 107006 (2008).

[36] S. Avci, O. Chmaissem, J. M. Allred, S. Rosenkranz, I. Eremin, A. V. Chubukov, D. E. Bugaris, D. Y. Chung, M. G. Kanatzidis, J.-P Castellan, J. A. Schlueter, H. Claus, D. D. Khalyavin, P. Manuel, A. Daoud-Aladine, and R. Osborn, Nat. Commun. **5**, 3845 (2014).

[37] F. Waßer, A. Schneidewind, Y. Sidis, S. Wurmehl, S. Aswartham, B. Büchner, and M. Braden, Phys. Rev. B **91**, 060505 (2015).

[38] J. M. Allred, K. M. Taddei, D. E. Bugaris, M. J. Krogstad, S. H. Lapidus, D. Y. Chung, H. Claus, M. G. Kanatzidis, D. E. Brown, J. Kang, R. M. Fernandes, I. Eremin, S. Rosenkranz, O. Chmaissem, and R. Osborn, Nat. Phys. **12**, 493 (2016).

[39] A. S. Sefat, R. Jin, M. A. McGuire, B. C. Sales, D. J. Singh, and D. Mandrus, Phys. Rev. Lett. **101**, 117004 (2008).

[40] L. J. Li, Y. K. Luo, Q. B. Wang, H. Chen, Z. Ren, Q. Tao, Y. K. Li, X. Lin, M. He, Z. W. Zhu, G. H. Cao, and Z. A. Xu, New J. Phys. **11**, 025008 (2009).

[41] D. K. Pratt, M. G. Kim, A. Kreyssig, Y. B. Lee, G. S. Tucker, A. Thaler, W. Tian, J. L. Zarestky, S. L. Bud'ko, P. C. Canfield, B. N. Harmon, A. I. Goldman, and R. J. McQueeney, Phys. Rev. Lett. **106**, 257001 (2011).

[42] X. Y. Lu, H. Gretarsson, R. Zhang, X. R. Liu, H. Q. Luo, W. Tian, M. Laver, Z. Yamani, Y.-J. Kim, A. H. Nevidomskyy, Q. Si, and P. C. Dai, Phys. Rev. Lett. **110**, 257001 (2013).

[43] S. Jiang, H. Xing, G. F. Xuan, C. Wang, Z. Ren, C. M. Feng, J. H. Dai, Z. A. Xu, and G. H. Cao, J. Phys.: Condens. Matter **21**, 382203 (2009).

[44] T. Shibauchi, A. Carrington, and Y. Matsuda, Annu. Rev. Condens. Matter Phys. **5**, 113 (2014).

[45] D. Hu, X. Y. Lu, W. L. Zhang, H. Q. Luo, S. L. Li, P. P. Wang, G. F. Chen, F. Han, S. R. Banjara, A. Sapkota, A. Kreyssig, A. I. Goldman, Z. Yamani, Ch. Niedermayer, M. Skoulatos, R. Georgii, T. Keller, P. S. Wang, W. Q. Yu, and P. C. Dai, Phys. Rev. Lett. **114**, 157002 (2015).

[46] A. D. Christianson *et al.*, Nature (London) **456**, 930 (2008).

[47] M. D. Lumsden, A. D. Christianson, D. Parshall, M. B. Stone, S. E. Nagler, G. J. MacDougall, H. A. Mook, K. Lokshin, T. Egami, D. L. Abernathy, E. A. Goremychkin, R. Osborn, M. A. McGuire, A. S. Sefat, R. Jin, B. C. Sales, and D. Mandrus, Phys. Rev. Lett. **102**, 107005 (2009).

[48] S. Chi, A. Schneidewind, J. Zhao, L. W. Harriger, L. J. Li, Y. K. Luo, G. H. Cao, Z. A. Xu, M. Loewenhaupt, J. P. Hu, and P. C. Dai, Phys. Rev. Lett. **102**, 107006 (2009).

[49] M. Wang, C. L. Zhang, X. Y. Lu, G. T. Tan, H. Q. Luo, Y. Song, M. Y. Wang, X. T. Zhang, E. A. Goremychkin, T. G. Perring, T. A. Maier, Z. Yin, K. Haule, G. Kotliar, and P. C. Dai, Nat. Commun. **4**, 2874 (2013).

[50] C. H. Lee, P. Steffens, N. Qureshi, M. Nakajima, K. Kihou, A. Iyo, H. Eisaki, and M. Braden, Phys. Rev. Lett. **111**, 167002 (2013).

[51] D. Hu, Z. P. Yin, W. L. Zhang, R. A. Ewings, K. Ikeuchi, M. Nakamura, B. Roessli, Y. Wei, L. X. Zhao, G. F. Chen, S. L. Li, H. Q. Luo, K. Haule, G. Kotliar, and P. C. Dai, Phys. Rev. B **94**, 094504 (2016).

[52] A. E. Böhmer, P. Burger, F. Hardy, T. Wolf, P. Schweiss, R. Fromknecht, H. V. Löhneysen, C. Meingast, H. K. Mak, R. Lortz, S. Kasahara, T. Terashima, T. Shibauchi, and Y. Matsuda, Phys. Rev. B **86**, 094521 (2012).

[53] See Supplemental Material at http://link.aps.org/supplemental/10.1103/PhysRevB.96.180503 for a detailed discussion.

[54] Yu Li, W. Y. Wang, Y. Song, H. Man, X. Y. Lu, F. Bourdarot, and P. C. Dai, Phys. Rev. B **96**, 020404(R) (2017).